

Confined Vortex Surface and Irreversibility. 2. Turbulent statistics

Alexander Migdal

*Department of Physics, New York University
726 Broadway, New York, NY 10003*

We study the Confined Vortex Surfaces (CVS) statistical distribution that we introduced in the previous paper. We use dilute gas approximation for the vorticity structures in a turbulent flow, assuming their size is much smaller than the mean distance between them. We justify the random Gaussian matrix strain model created as a background for each vortex surface from the sea of other surfaces far away. We compute this self-consistent background strain, relating the variance of the strain to the energy dissipation rate. In the end, we find a universal asymmetric distribution for the energy dissipation, sharply decreasing on both ends.

1. Introduction

The ultimate goal of turbulence studies is to solve the Navier-Stokes equations and find out how and why the solution covers some manifold rather than staying unique given initial data and boundary conditions.

We also need to understand why it is irreversible even in the limit of zero viscosity when the Navier-Stokes equations formally become the Euler equation corresponding to the reversible Hamiltonian system with conserved energy.

Once we know why and how, we would like to know all the properties of this manifold – what are the parameters, what is the invariant measure on this manifold, and how the observables like the energy dissipation rate are distributed.

The first obstacle to overcome on this path is to understand the irreversibility of the Navier-Stokes dynamics in a limit when viscosity goes to zero at fixed energy dissipation.

We know (or at least we assume) that the vortex structures in this extreme turbulent flow are not uniformly spread over space. Snapshots of vorticity in numerical simulations show a collection of tube-like structures relatively sparsely distributed in space.

Such 2D structures are known in the Euler dynamics: these are vortex surfaces. Vorticity collapses into a thin boundary layer around the surface, making the problem look like a problem of random surfaces moving in the own velocity field. Such motion is known to be unstable against the Kelvin-Helmholtz instabilities, which undermines the whole idea of random vortex surfaces.

However, exact solutions of the Navier-Stokes equations discovered in the previous century by Burgers and Townsend^{1,2} show stable planar sheets with

Gaussian profile of the vorticity in the normal direction. This nice Gaussian solution is not the most general one; it takes some tuning parameters in the background flow.

The recent research^{3,4} revealed that the Burgers-Townsend regime required vanishing eigenvalue of the strain, plus the negative value of the normal component of the strain.

Abstracting from these observations, we conjectured⁵ that the stability condition of the vortex surface is given by two equations

$$\hat{S} \cdot \Delta \vec{v} = 0; \quad (1)$$

$$S_{nn} = \vec{\sigma} \cdot \hat{S} \cdot \vec{\sigma} < 0 \quad (2)$$

The first condition is an enhanced version of the vanishing eigenvalue requirement. The velocity gap Δv should be a null vector of this zero eigenvalue, which is stronger than demanding $\det \hat{S} = 0$.

As for the second requirement, with $\vec{\sigma}$ being the local normal vector, it demands that the strain pushes the fluid towards the surface on both sides.

With negative normal strain and zero strain in direction of velocity gap, the flow effortlessly slides along the surface on both sides, without leakage and pile-up.

This is an intuitive explanation of the CVS conditions– they provide the permanent tangential flow around the surface, confining vorticity inside the boundary layer.

Once these requirements are satisfied in the local tangent plane, one could solve the Navier-Stokes equation in the boundary layer and obtain the Gaussian Burgers-Townsend solution, vindicating the stability hypothesis. An error function of normal coordinate will replace the velocity gap, and the delta function in tangent vorticity will become the Gaussian profile with viscous width.

With inequality satisfied, this width will be real positive

$$h = \sqrt{\frac{v}{-S_{nn}}} \quad (3)$$

It is important to understand that this inequality breaks the reversibility of the Euler equation: the strain is an odd variable for time reflection, although it is even for space reflection.

This stability requirement is a dynamic mechanism of the irreversibility of the turbulent flow: the vorticity can collapse only to the surface with negative normal strain.

2. The exact solution

In the first part of this study⁵ we have found an analytic solution for the Euler equations with additional CVS constraints in the presence of an arbitrary constant strain.

Let us describe this solution before studying the associated turbulent statistics.

The steady closed vortex surface \mathcal{S} can be treated within the framework of hydrostatics, as it was recently advocated in our paper.³

In the 3D space inside and outside the surface $\mathcal{S}^\pm : \partial\mathcal{S}^\pm = \mathcal{S}$ there is no vorticity, so the flow can be described by a potential $\Phi_\pm(\vec{r})$

$$v_\alpha(\vec{r}) = \partial_\alpha \Phi_\pm(\vec{r}); \forall \vec{r} \in \mathcal{S}^\pm \quad (4)$$

The incompressibility $\partial_\alpha v_\alpha = 0$ would be satisfied provided both potentials satisfied Laplace equation with the Neumann boundary conditions at the surface

$$\partial_\alpha v_\alpha(\vec{r}) = \partial_\alpha^2 \Phi_\pm(\vec{r}) = 0; \forall \vec{r} \in \mathcal{S}^\pm \quad (5)$$

$$\partial_n \Phi_+(\vec{r}) = \partial_n \Phi_-(\vec{r}); \forall \vec{r} \in \mathcal{S} \quad (6)$$

The pressure in each of the domains inside/outside is given by the Bernoulli formula

$$p_\pm = -\frac{1}{2} (\partial_\alpha \Phi_\pm(\vec{r}))^2 \quad (7)$$

The tangent velocity gap $\Delta\vec{v}$ arises because of the gap in the potential

$$\Gamma = \Phi_+(\vec{r}) - \Phi_-(\vec{r}); \forall \vec{r} \in \mathcal{S}; \quad (8)$$

$$\Delta\vec{v} = \vec{\nabla}\Gamma \quad (9)$$

Our solution has the form of parametrization of complex velocity field and the complex xy coordinate by two holomorphic functions $V(\xi), C(\xi)$ outside the unit disk in complex plane ξ .

$$v_z = -2pz; \quad (10a)$$

$$v_x - \imath v_y = (p+q)x + \imath(q-p)y + qR_0\theta(|\xi| - 1)V(\xi) \quad (10b)$$

$$x + \imath y = R_0C(\xi); \quad (10c)$$

$$\Phi_+(x, y, z) = \frac{(p+q)x^2 + (p-q)y^2 - 2pz^2}{2} + qR_0^2 \frac{\gamma \arg \xi}{2\pi}; \quad (10d)$$

$$\Phi_-(x, y, z) = \frac{(p+q)x^2 + (p-q)y^2 - 2pz^2}{2}; \quad (10e)$$

$$V(\xi) = \frac{\gamma}{2\pi\imath \xi C'(\xi)}; \quad (10f)$$

The CVS equations (1) reduce to the following relations for differentials of these functions on the unit circle

$$2dC(pV + qV^*) + V^*dV = 0; \quad (11)$$

$$VdC = \frac{\gamma}{2\pi}d\theta; \quad (12)$$

$$\xi = \exp(\imath\theta); \quad (13)$$

Here γ is an arbitrary real parameter, proportional to the velocity circulation around the cylindrical surface, i.e., the vorticity flux through its skin in the axial direction.

As it was discussed in previous paper⁵ the Burgers-Townsend planar vortex sheet is recovered in the singular limit $p \rightarrow -q, \gamma \rightarrow \infty$, when $V(\xi) \rightarrow \Delta v_x = \text{const}$. The parametric equation $C(\xi) \rightarrow \frac{\gamma}{2\pi\Delta v_x}\theta$ becomes equation for the growing interval on the real axis becoming the whole real axis at $\gamma = \infty$.

Let us come back to the general case of arbitrary p, q in the physical interval $-q < p < 0$.

The CVS equations are invariant under the scale transformations

$$V \Rightarrow \lambda V; \quad (14)$$

$$C \Rightarrow \lambda C; \quad (15)$$

$$\gamma \Rightarrow \lambda^2 \gamma; \quad (16)$$

which we fixed by introducing the scale parameter R_0 in our solution and imposing the normalization condition

$$\mathbf{Im} V(\xi = i) = 1; \quad (17)$$

The normal strain for our cylindrical solution is constant

$$S_{nn} = 2p \quad (18)$$

At $-q < p < 0$ we have negative strain as required by the stability of the Navier-Stokes equation in the local tangent plane. The solution depends on dimensionless parameter varying between 0 and 1.

$$\mu = \frac{q+p}{q-p}; \quad (19)$$

$$\mu \in (0, 1); \quad (20)$$

The function $C(\xi)$ are given by integral

$$C(\xi) = \frac{\xi^3(\mu+1)}{2\gamma} \int_1^{v_2} \frac{dv}{v} (u^2 + v^2) \left(\frac{(x+iy)\omega^*(v)}{\omega(v)^2 - \xi^2} + \frac{(x-iy)\omega(v)}{\omega^*(v)^2 - \xi^2} \right); \quad (21a)$$

The functions and parameters here are defined as

$$\kappa = \sqrt{\mu} \frac{\sqrt{\frac{2}{1+\mu}\gamma - v_2^2 + 1}}{\sqrt{1 - v_2^{-2\mu}}}; \quad (22a)$$

$$\theta(v) = \pi \frac{1+\mu}{2\mu\gamma} \left(\mu(v_2^2 - v^2) + \kappa^2 (v^{-2\mu} - v_2^{-2\mu}) \right); \quad (22b)$$

$$\omega(v) = \exp(i\theta(v)); \quad (22c)$$

$$u = \kappa v^{-\mu}; \quad (22d)$$

$$x + iy = \frac{1+\mu}{2\mu} (\kappa - u + i\mu(v_2 - v)); \quad (22e)$$

Directly at the unit circle

$$C\left(\exp(i\theta(v))\right) = \frac{(\mu+1)\left(\kappa(v^{-\mu}-1) + i\mu(v-v_2)\right)}{4\mu}; \forall 1 < v < v_2 \quad (23)$$

Finally there are two transcendental equations for two free parameters γ, v_2

$$C(1) = -\frac{(\mu+1)\kappa\left(1-v_2^{-\mu}\right)}{4\mu}; \quad (24a)$$

$$C(i) = -i\frac{(\mu+1)(v_2-1)}{4}; \quad (24b)$$

These equations are needed for the four separate segments of the loop (each for each quadrant of the unit circle ζ) to match each other at the boundaries between the quadrants, closing the loop.

The velocity gap at the loop $V(\zeta), |\zeta| = 1$ is not continuous at $\zeta = \pm 1, \zeta = \pm i$. The absolute value of $V(\zeta)$ stays continuous at these four points but the phase (i.e., the direction of velocity gap) changes, following the cusps of the boundary curve $C(\zeta)$.

The flow everywhere outside the surface is finite with all derivatives, and the singular part decreases as $1/|x+iy|$.

There are also two parameters of translation of this cylindrical surface in xy plane, plus three parameters of rotation of the coordinate system, which we chose to coincide with eigenvectors of the background strain $W = \text{diag}((p+q), (p-q), -2p)$.

3. The induced background strain

What is the physical origin of the constant background strain $W_{\alpha\beta}$ which we used in our solution?

Traditionally, the ad-hoc Gaussian random forces are added to the Navier-Stokes equation to simulate the effects of the unknown inner randomness.

We do not think that this beautiful equation needs any crutches; it can walk all by itself.

In our theory, the random forces come from the multitude of remote vortex structures, contributing to the background velocity field via the Biot-Savart law.

These forces are not arbitrary; they are rather self-consistent, like a mean-field in the ordinary statistical mechanics.

Let us assume that space is occupied by some localized CVS structures far from each other. In other words, let us consider an ideal gas of vortex bubbles.

This ideal gas approximation is close to reality, where the vorticity occupies a small subset of the physical space with fractal dimension^{6,7} $D_f \approx \frac{7}{3} < 3$.

In such an ideal gas, one can neglect the collision of particles, which in our case is a nontrivial matter, with vortex surfaces avoiding each other.

While neglecting the collisions of vortex structures, we still cannot neglect the long-range effect of the strain they impose on each other.

The Biot-Savart formula for the velocity field induced by the set of remote localized vorticity bubbles B

$$\vec{v}(\vec{r}) = \sum_B \int_B d^3r' \frac{\vec{\omega}(\vec{r}') \times (\vec{r}' - \vec{r})}{4\pi|\vec{r} - \vec{r}'|^3} \quad (25)$$

falls off as $1/r^2$ for each bubble, like an electric field from the charged body.

Note that all the vortex structures in the volume contribute to this background velocity field, adding up from a large number of small terms at every point in space.

If there are many such bubbles distributed in space with small but finite density, we would have the "night sky paradox." The bubbles spread on the far away sphere will compensate the inverse distance squared to have a divergent distribution like $\int R^2 dR/R^2$. (see Fig. 5).

This estimate is, of course, wrong, as the directions of velocity contributions from various bubbles are uncorrelated, so there is no coherent mean velocity.

Also, a Galilean transformation would remove the finite background velocity, so it does not lead to any physical effects.

However, with the strain, there is another story. Strain coming from remote vortex bubbles

$$W_{\alpha\beta}(\vec{r}) = e_{\alpha\mu\gamma} \partial_\beta \partial_\gamma \sum_B \int_B d^3r' \frac{\omega_\mu(\vec{r}')}{4\pi|\vec{r} - \vec{r}'|} \quad (26)$$

falls off as $1/r^3$, and this time, there could be a mean value \bar{W} , coming from a large number of random terms from various bubbles with distribution $R^2 dR/R^3 \sim dR/R$.

The space symmetry arguments plus some more refined arguments we present in the next section tell us that averaging over the directions of the bubble centers $\vec{R} = \vec{r}' - \vec{r}$ completely cancels this mean value.

The Central Limit Theorem suggests (within our ideal vortex gas model) that such a strain would be a Gaussian tensor variable, satisfying the normal distribution of a symmetric traceless matrix with zero mean

$$dP_\sigma(W) \propto \prod_i dW_{ii} \prod_{i<j} dW_{ij} \delta\left(\sum_i W_{ii}\right) \exp\left(-\frac{\text{tr } W^2}{2\sigma^2}\right) \quad (27)$$

This distribution was studied extensively in physics and mathematics, so we are not giving references here. Separating O_3 rotations $\Omega \in S_2$, we have the measure for eigenvalues $p + q, p - q, -2p$:

$$dP_\sigma(W) = \frac{1}{4\pi} d\Omega dp dq P_\sigma(p, q); \quad (28)$$

$$P_\sigma(p, q) = 4\sqrt{\frac{3}{\pi}} \theta(q) \theta(p+q) \theta(-p) q |q^2 - 9p^2| \exp\left(-\frac{3p^2 + q^2}{\sigma^2}\right) \quad (29)$$

In our case, we are interested in the region $-q < p < 0$, where the vortex surface is stable.

4. Energy dissipation

The general formula⁵ for the surface dissipation reads

$$\mathcal{E} = \frac{\sqrt{v}}{2\sqrt{2\pi}} \int_D d^2\xi \sqrt{g} \sqrt{-S_{nm}} (\vec{\nabla}\Gamma)^2; \quad (30)$$

As we noticed in the previous work⁵ this surface dissipation is conserved on CVS surfaces.

Without CVS as a stability condition, the dissipation itself would not be an integral of motion, undermining the hypothesis of the steady energy flow, which is central to any modern theory or model of turbulence.

For our solution the energy dissipation integral takes the form of scaling law

$$\frac{\mathcal{E}}{L\sigma\sqrt{v}\Delta\Gamma^{\frac{3}{2}}} = \frac{q}{\sigma} F(\mu); \quad (31)$$

$$F(\mu) = \frac{\sqrt{1-\mu^2}}{2\sqrt{\pi}} \gamma(\mu)^{-\frac{3}{2}} \int_1^{v_2(\mu)} dv \frac{(u^2 + v^2)^{\frac{3}{2}}}{v} \quad (32)$$

where the functions $\gamma(\mu)$, $v_2(\mu)$ are computed in⁸ as functions of μ . The integral here can be expressed in terms of hypergeometric functions.

$$\int_1^{v_2(\mu)} dv \frac{(u^2 + v^2)^{\frac{3}{2}}}{v} = \frac{\kappa v_2^{-3\mu}}{9\mu} (F_1 + F_2 + F_3 + F_4); \quad (33)$$

$$F_1 = \left(\kappa^2(\mu + 4) - 2\mu + 1 \right) v_2^{3\mu} {}_2F_1 \left(-\frac{1}{2}, -\frac{3\mu}{2\mu + 2}; \frac{2 - \mu}{2\mu + 2}; -\frac{1}{\kappa^2} \right); \quad (34)$$

$$F_2 = -(\mu + 1) (\kappa^2 + 1) v_2^{3\mu} {}_2F_1 \left(\frac{1}{2}, -\frac{3\mu}{2\mu + 2}; \frac{2 - \mu}{2\mu + 2}; -\frac{1}{\kappa^2} \right); \quad (35)$$

$$F_3 = +(\mu + 1) (\kappa^2 + v_2^{2\mu+2}) {}_2F_1 \left(\frac{1}{2}, -\frac{3\mu}{2\mu + 2}; \frac{2 - \mu}{2\mu + 2}; -\frac{v_2^{2\mu+2}}{\kappa^2} \right); \quad (36)$$

$$F_4 = \left((2\mu - 1)v_2^{2\mu+2} - \kappa^2(\mu + 4) \right) {}_2F_1 \left(-\frac{1}{2}, -\frac{3\mu}{2\mu + 2}; \frac{2 - \mu}{2\mu + 2}; -\frac{v_2^{2\mu+2}}{\kappa^2} \right) \quad (37)$$

This universal function $F(\mu)$ is shown at Fig. 3.

It vanishes at $\mu = 1$, which is the end of the stability region.

The Gaussian matrix integral we presented in the previous section transforms to depend on μ, q with probability density

$$P_{\mu q}(\mu, q) = \frac{64\sqrt{\frac{3}{\pi}}(2 - \mu)q^4|2\mu - 1|e^{-\frac{4((\mu-1)\mu+1)q^2}{(\mu+1)^2}}}{(\mu + 1)^4} \quad (38)$$

We measure q in units of the Gaussian variance σ .

The resulting distribution for the scaling variable takes the form

$$\zeta = \frac{\mathcal{E}}{L\sqrt{\nu}\sigma(\Delta\Gamma)^{\frac{2}{3}}}; \quad (39)$$

$$P(\zeta) = \int_0^1 d\mu F(\mu) P_{\mu q} \left(\mu, \frac{\zeta}{F(\mu)} \right) \quad (40)$$

We coded these formulas in.⁸

Here is the resulting curve for $P(\zeta)$ in log-log scale(Fig. 4).

The mean value of the energy dissipation is

$$\langle \zeta \rangle = \frac{\int P(\zeta) \zeta d\zeta}{\int P(\zeta) d\zeta} = 0.186671 \quad (41)$$

With log-log plot, the shape of the curve does not depend on the normalization of variables, so it is completely universal. It would be extremely interesting to compare that with DNS.

One could regard these formulas as distribution of the circulation $\Delta\Gamma$ at fixed energy dissipation rate. The obvious change of variables converts the above PDF into the PDF for

$$\lambda = \Delta\Gamma \left(\frac{L\sqrt{\nu}\sigma}{\mathcal{E}} \right)^{\frac{2}{3}}; \quad (42)$$

5. Energy

Let us now compute the energy of the vortex surface as a Hamiltonian system.^{6,7} There is a regular part related to the background strain. This part is not involved in the minimization we are interested in; it depends on p, q , which are external parameters for our problem.

The internal part of the Hamiltonian is directly related to the potential gap Γ we have computed in the previous section.

$$H_{int} = \int_{\vec{r}_1, \vec{r}_2 \in \mathcal{S}} d\Gamma(\vec{r}_1) \wedge d\vec{r}_1 \cdot d\Gamma(\vec{r}_1) \wedge d\vec{r}_1 \frac{1}{8\pi|\vec{r}_1 - \vec{r}_2|} \quad (43)$$

In our case of cylindrical surface

$$d\Gamma(\vec{r}_1) \wedge d\vec{r}_1 = d\Gamma(\theta) \{0, 0, dz\} \quad (44)$$

and we have a separation of variables θ, z .

The integration over z_1, z_2 provides the total length $L \rightarrow \infty$ of the cylinder times logarithmically divergent integral over $z_1 - z_2$. We limit this integral to the

interval $(-L, L)$ and compute it exactly

$$\int_{-L}^L \frac{1}{8\pi\sqrt{\eta^2 + z^2}} dz = \frac{\log\left(\frac{2L(\sqrt{\eta^2 + L^2} + L)}{\eta^2} + 1\right)}{8\pi} \quad (45)$$

Then we expand it at large L

$$\int_{-L}^L \frac{1}{8\pi\sqrt{\eta^2 + z^2}} dz \rightarrow \frac{\log(2L) - \log|\eta|}{4\pi} + O\left(\frac{\eta^2}{L^2}\right) \quad (46)$$

Thus we get in our case, with $\Delta\Gamma = qR_0^2\gamma(\mu)$

$$\begin{aligned} \frac{H_{int}}{L} &= \log(2L/R_0) \frac{(\Delta\Gamma)^2}{4\pi} \\ &- \frac{(\mu+1)^2(\Delta\Gamma)^2}{8\pi R_0 \gamma^2(\mu)} \int_1^{v_2(\mu)} \frac{dw_1}{w_1} \int_1^{v_2(\mu)} \frac{dw_2}{w_2} (\kappa^2 w_1^{-2\mu} + w_1^2)(\kappa^2 w_2^{-2\mu} + w_2^2) \\ &\log\left|(C^2(w_1) - C^2(w_2))(C^2(w_1) - (C^*(w_2))^2)\right|; \end{aligned} \quad (47)$$

$$R_0 = \sqrt{\frac{\Delta\Gamma}{q\gamma(\mu)}} \quad (48)$$

Here we should use the parametrization (21) for the loop C in the first quadrant.

The logarithmic divergence of the leading term makes it unphysical. Unlike energy dissipation, which is finite and conserved, the energy is divergent and not conserved.

The same was true in traditional Kolmogorov theory, where the energy diverged because of the growing velocity correlations in physical space, or the infrared-divergent spectrum $dk|k|^{-\frac{5}{3}}$ in the Fourier space.

6. Dilute gas of vortex bubbles in mean-field approximation

Let us elaborate on this idea of a dilute gas of vortex bubbles and compute the strain variance.

Consider a large number of independent vortex bubbles, sparsely distributed in the 3D volume.

The net strain at the vicinity of this surface will come from the Biot-Savart formula, which we expand at large distances (plus symmetric terms with swapped α, β)

$$\begin{aligned} W_{\alpha\beta}(\vec{r}) &\rightarrow \\ e_{\alpha\mu\gamma} \left(\Omega_\mu \partial_\beta \partial_\gamma + \Omega_{\mu\lambda} \partial_\beta \partial_\gamma \partial_\lambda + \dots \right) \frac{1}{4\pi|\vec{r}|}; \end{aligned} \quad (49)$$

$$\Omega_\mu = \int_B d^3 r' \omega_\mu(\vec{r}'); \quad (50)$$

$$\Omega_{\mu\lambda} = \int_B d^3 r' \omega_\mu(\vec{r}') r'_\lambda \quad (51)$$

The contribution to the strain from each remote vortex blob will be linearly related to its net vorticity vector Ω_μ .

These vectors are randomly distributed with zero mean^a, in addition to the random locations on a sphere which is why we expect the Central Limit Theorem to apply here (see Fig. 5).

The vorticity for each vortex bubble S is given by a surface integral^{6,7}

$$\omega_v(\vec{r}) = \int_S d\Gamma \wedge dr'_v \delta^3(\vec{r} - \vec{r}'); \quad (52)$$

$$\Omega_\mu = \int_S d\Gamma \wedge dr_\mu; \quad (53)$$

$$\Omega_{\mu\lambda} = \int_S d\Gamma \wedge dr_\mu r_\lambda \quad (54)$$

Averaging over directions of the position vector \vec{r} of the bubble on the sphere centered at this surface, we get exactly zero. We verified that up to the fourth term by symbolic integration.⁹ There is, of course, a general reason for these cancellations.

The rotational average of the multiple derivative matrix has only one totally symmetric symmetric tensor structure

$$\begin{aligned} T_{\mu_1 \dots \mu_n} &= \left\langle \partial_{\mu_1} \dots \partial_{\mu_n} \frac{1}{|\vec{r}|} \right\rangle_{\vec{r} \in S_2} = \\ &= C \left(\delta_{\mu_1 \mu_2} \dots \delta_{\mu_{n-1} \mu_n} + \text{permutations} \right) \end{aligned} \quad (55)$$

However, the contraction over any pair of indices yields zero because $\frac{1}{|\vec{r}|}$ satisfies the Laplace equation. Therefore $C = 0$.

The number dN of the vortex structures on the large sphere would be estimated as

$$dN = 4\pi\rho(R)R^2 dR \quad (56)$$

where $\rho(R)$ is the distribution of distances between the vortex structures.

This produces the formula for σ with separated averaging over the unit vector on a sphere S_2 and the random tensor W

$$5\sigma^2 = \frac{1}{\pi^2} \left\langle \Omega_\mu^2 \right\rangle_W \int dR \frac{\rho(R)}{R^4}; \quad (57)$$

This distribution is normalized as

$$4\pi \int dR \rho(R) R^2 = 1 \quad (58)$$

^aThe directions of these vectors in our exact solution coincide with one of the eigenvectors of the local strain tensor at the location of that particular CVS surface. Assuming these locations to be randomly distributed in space, so will be the strain tensors and so will be the vorticity vectors (directed along the symmetry axis of the cylindrical solution).

Therefore, our expression involves a mean value of $1/R^6$

$$\left\langle \frac{1}{R^6} \right\rangle = \frac{\int dR \rho(R) R^{-4}}{\int dR \rho(R) R^2}; \quad (59)$$

$$\int dR \rho(R) R^{-4} = \frac{1}{4\pi} \left\langle \frac{1}{R^6} \right\rangle \quad (60)$$

After that, we relate the variance to the mean squared vorticity of each vortex structure and the relative distance distribution of these tubes.

$$\sigma^2 = \frac{1}{20\pi^3} \left\langle \Omega_\alpha^2 \right\rangle_W \left\langle \frac{1}{R^6} \right\rangle \quad (61)$$

In our theory, with cylindrical tube of size L

$$\Omega_\alpha = \delta_{\alpha 3} L \Delta \Gamma \quad (62)$$

So, we find the following expression for the variance of strain

$$\sigma^2 = \frac{1}{20\pi^3} \frac{\left\langle L^2 \Delta \Gamma^2 \right\rangle}{\bar{R}^6}; \quad (63)$$

$$\bar{R} = \left\langle \frac{1}{R^6} \right\rangle^{-\frac{1}{6}} \quad (64)$$

This brings us to the final result for the mean energy dissipation

$$\left\langle \frac{\mathcal{E}}{L(\Delta \Gamma)^{\frac{3}{2}}} \right\rangle = 0.00749613 \frac{\sqrt{\nu \left\langle L^2 \Delta \Gamma^2 \right\rangle}}{\bar{R}^3} \quad (65)$$

Thus, we got a scaling relation in the turbulent limit

$$\nu(\Delta \Gamma)^5 \bar{R}^{-6} L^2 \sim \left(\frac{\mathcal{E}}{L} \right)^2 = \text{const} \quad (66)$$

The dissipation per unit length $\frac{\mathcal{E}}{L}$ is expected to stay finite in the turbulent limit $\nu \rightarrow 0$. Our previous conjecture^{10,11} was: the geometry stays finite, and the velocity (i.e.) $\Delta \Gamma$ grows as $\nu^{-\frac{1}{5}}$ to keep the left side finite in the turbulent limit.

However, now we see more natural possibility:

$$L \sim \nu^{-\frac{1}{2}} \rightarrow \infty \quad (67)$$

and everything else stays finite.

This limit solves all the problems. At the same time, it vindicates our assumption of cylindrical geometry. The growing length L of the cylinder is the only way to keep the energy dissipation finite, with other observables staying finite as well.

7. Ginsburg-Landau effective Hamiltonian for the induced strain

The exact solution for the cylindrical surface we have found in⁵ does not depend on the axial coordinate z of the cylinder. From the point of view of the mean-field theory, this is just an approximation.

The radial size of our tube is supposedly small compared to the average distance between vortex structures in a turbulent flow which is why we neglected the variation of the induced background strain over the cross-section of our tube.

However, when we move in the longitudinal direction z of the tube on the distance comparable with the mean distance between vortex blobs, this induced strain will change.

The same approximation of constant local strain will apply to the vortex surface equations, with changed background strain W . Thus, we will have the above solution for the vortex surface, and its flow slowly evolve.

The frame where the strain is diagonal will slowly rotate, and so our tube will start to bend and rotate, following the eigenvectors of the slowly varying induced local strain.

The resulting surface will look like this (Fig.6).

The eigenvalues $p + q, p - q, -2p$ of the strain, which determines the shape of the vortex surface and its flow, will also start slowly varying in space. Presumably, at the endpoints of the tube, the requirement $p < 0$ breaks, leading to a singular tip.

We have heard this tune before. The Landau-Ginsburg theory of phase transitions, with the order parameter (background strain in our case), slowly varying in space.

The effective Landau-Ginsburg field theory suggests the distribution of this order parameter

$$D\hat{W}\delta(\text{tr } \hat{W}) \exp\left(-\int d^3r \text{tr } U(\hat{W}) + \frac{1}{2}\kappa(\partial_\mu W_{\alpha\beta})^2\right) \quad (68)$$

with some large parameter $\kappa \sim R^2$ related to the large distance between vortex structures. In the limit of $\kappa \rightarrow \infty$ the field \hat{W} would become a uniform random traceless symmetric matrix with some expectation value.

This expectation value will be degenerate, as the potential is rotation invariant. Thus, we will have essentially the same model as above, with random rotation matrices and eigenvalues distributed around the minimum of the potential.

Such theories were extensively studied in the modern theory of critical phenomena. Neglecting the spatial variations, we have essentially the same classical theory, with the extra complication that we have to solve the CVS equations for the vortex surface in the presence of this random background strain.

Something has to be corrected here. As we are using the strain in the potential

$$\Phi(\vec{r}) = \frac{1}{2}r_\alpha r_\beta W_{\alpha\beta} \quad (69)$$

we do not want to break the Laplace equation (i.e. incompressibility of the potential flow).

For that end the strain has to satisfy the condition

$$\partial_\alpha V_\alpha = 0; \quad (70)$$

$$V_\alpha = \partial_\alpha \Phi = r_\beta W_{\alpha\beta} + \frac{1}{2} r_\mu r_\nu \partial_\alpha W_{\mu\nu} \quad (71)$$

This condition requires another field, the Lagrange multiplier

$$D\hat{W}\delta(\text{tr } \hat{W})D\Lambda \exp\left(-\int d^3r \text{tr } U(\hat{W}) + \iota V_\alpha \partial_\alpha \Lambda + \frac{1}{2} \kappa (\partial_\mu W_{\alpha\beta})^2\right) \quad (72)$$

One can use such a local strain to replace the constant strain in our potential solutions. The Gaussian functional integral here would lead to calculable terms of the perturbative expansion around a uniform random matrix W .

This method is similar to the Wylde functional integral, with the second field introduced as a Lagrange multiplier for the equations of motion.

There are two independent components of a traceless symmetric tensor apart from the rotations. This extra constraint eliminates one degree of freedom, leaving one independent invariant. In practice, there is no need to solve this constraint as the Gaussian functional integral is calculable in a general form.

This approach could lead to the quantitative description of the observed cylindrical vortex tubes¹² which are bending and twisting in the turbulent flow and terminating with cusps.

At the moment, this is just wishful thinking, but we feel it important to point out this possible direction for future research.

8. Wilson Loop Statistics

Let us assume that we have some CVS surface parameterized by p, q in the random tensor $W = \text{diag}(p + q, p - q, -2p)$.

There are space translations, factored by a cylindrical translation in the z axis and parameters of the symmetric traceless matrix W : two eigenvalues p, q plus arbitrary rotations of the coordinate system,

As we described in the previous sections, we treat this W as the background uniform strain created by other vortex structures far away from the surface's axis. One would think that this strain, adding up strains from a large number of randomly positioned vortex structures like this one, would be a random traceless symmetric tensor.

However, only a negative sign of p leads to the negative normal strain, as required by our theory.

Here is a subtle point. The random strain distribution at infinity does not "know" it has to create the stable vortex sheet. What happens in these (equally probable) cases when the strain is positive?

We answer that there will be no stable vortex surface in this region in these cases – the background vorticity would stay at a constant level and will not collapse into the vortex surface. Such collapse can only happen for the negative strain at the surface.

We are left with an integral over zero modes: translation and rotation of the coordinate system plus two eigenvalues of the random constant strain at infinity. We should integrate over these parameters the observables computed for a particular solution of *CVS*.

To be specific, let us consider the loop average

$$W_C(\gamma) \propto \int d^3r_0 d\Omega dP(p, q) \exp\left(i\gamma \oint_C v_\alpha(\vec{r}) dr_\alpha\right) \quad (73)$$

The velocity circulation in the exponential comes only from the intersection points of the loop C with our cylindrical surface. A simple loop intersects the surface in two points or does not intersect at all, so we have

$$\Gamma_{12} = \oint_C v_\alpha dr_\alpha = \mathbf{Re} (f(\eta_2) - f(\eta_1)) \quad (74)$$

The integral here goes along the path connecting two intersection points $\eta_1, \eta_2 \in C$ where we know the surface equation from our exact solution. The circulation is especially simple: it is proportional to the angle on the unit circle in ζ plane

$$\Gamma_{12} = \Delta\Gamma \frac{\theta_2 - \theta_1}{2\pi}; \quad (75)$$

Thus, up to extra terms independent of γ

$$W_C(\gamma) \propto \int d^3r_0 d\Omega dP(a, b) \Pi_S(\vec{r}_0, \Omega, \gamma) \quad (76)$$

The factor

$$\begin{aligned} \Pi_S(\vec{r}_0, \Omega, \gamma) &= \int_0^1 dl_1 |C'(l_1)| \int_0^1 dl_2 |C'(l_2)| \\ &\int_{\vec{r}_1 \in S} \int_{\vec{r}_2 \in S} \delta^3(\vec{r}_1 + \Omega \cdot (\vec{r}_0 - \vec{C}(l_1))) \delta^3(\vec{r}_2 + \Omega \cdot (\vec{r}_0 - \vec{C}(l_2))) \\ &\exp\left(i\gamma \Delta\Gamma \frac{\theta_2 - \theta_1}{2\pi}\right) \end{aligned} \quad (77)$$

was already computed in¹¹

$$\begin{aligned} \Pi_S(\vec{r}_0, \Omega, \gamma) &= \frac{|\vec{\sigma}_1| |C'(l_1)|}{|\vec{\sigma}_1 \cdot \Omega \cdot \vec{C}'(l_1)|} \frac{|\vec{\sigma}_2| |C'(l_2)|}{|\vec{\sigma}_2 \cdot \Omega \cdot \vec{C}'(l_2)|} \theta(\vec{r}_1 \in S) \theta(\vec{r}_2 \in S) \\ &\exp\left(i\gamma \Delta\Gamma \frac{\theta_2 - \theta_1}{2\pi}\right); \end{aligned} \quad (78)$$

$$\vec{\sigma}_1 = \vec{\sigma}(\vec{r}_1); \vec{\sigma}_2 = \vec{\sigma}(\vec{r}_2); \quad (79)$$

$$\vec{r}_1 = \Omega \cdot (\vec{C}(l_1) - \vec{r}_0); \vec{r}_2 = \Omega \cdot (\vec{C}(l_2) - \vec{r}_0); \quad (80)$$

This integral depends on the geometry of the problem: the relation between the loop C and the cylinder. The phase factor depends on the random strain parameters via known $\theta = \theta(v)$.

We are left with an integral over $2d$ translations \vec{r}_0 against the cylinder's axis and the O_3 rotations Ω .

The two theta functions, restricting the points to be on the intersection of the surface and the loop, are zero if the point \vec{r}_0 moves from the surface farther than the maximal size of the loop C .

The integration region for \vec{r}_0 is some layer around the vortex surface, with the width equal to the maximal distance between two points on the loop.

The integration over rotations Ω is compact. Therefore, this integral looks like a relatively straightforward integral from a computational point of view.

As we already mentioned, there is no time-reversal symmetry that would reflect γ . The flux $\Delta\Gamma$ is the same sign as q in our irreversible solution.

Therefore, our Wilson loop will be a complex number. Nobody has measured it in DNS, but its Fourier transform (over circulation, not over space coordinates) represents the circulation PDF measured with high accuracy.

This Fourier transform would simply mean replacement

$$\exp\left(i\gamma\Delta\Gamma\frac{\theta_2 - \theta_1}{2\pi}\right) \Rightarrow \delta\left(\Delta\Gamma\frac{\theta_2 - \theta_1}{2\pi} - \oint_C \vec{v} \cdot d\vec{r}\right) \quad (81)$$

This delta function is welcome, as it will reduce the dimension of the remaining integration over \vec{r}_0 .

After that, *Mathematica*[®] can compute this finite integral with arbitrary precision.

Another possibility is to compute the moments of the circulation $M_n = \left\langle \left(\oint_C \vec{v} \cdot d\vec{r}\right)^n \right\rangle$ which would correspond to the replacement

$$\exp\left(i\gamma\Delta\Gamma\frac{\theta_2 - \theta_1}{2\pi}\right) \Rightarrow \left(\Delta\Gamma\frac{\theta_2 - \theta_1}{2\pi}\right)^n \quad (82)$$

Thus, there is a steep but clear path to compute a Wilson loop using the above formulas. Multidimensional integrals can be computed by local adaptive subdivision¹³ rather than the Monte-Carlo method because the dimension of the integration is low and the functions are known analytically.

9. Discussion

This theory of vortex surfaces offers an approach to turbulence that one can study analytically and numerically.

Let us remind and discuss the general ideas behind this theory.

We are trying to solve the Navier-Stokes equations for an infinite time evolution, given that the laminar flow is unstable. This unstable solution could cover the whole phase space of the fluid mechanics; however, we expect that there are some attractors in that space.

We expect the solution to cover the subspace of these attractors like the Newtonian dynamics covers the energy surface in ergodic motion.

We also know the phenomenon of anomalous dissipation: the dissipation in extreme turbulence occurs in the regions of high vorticity, which compensates the viscosity factor in front of the enstrophy integral.

Furthermore, we conjecture that these regions of high vorticity are vortex surfaces. There are several reasons to believe so, both on the theoretical and (numerical or real) experimental side.

The Hamiltonian dynamics of vortex surfaces^{6,7} can be solved exactly in some important cases, and the resulting solutions have all nice properties, including anomalous dissipation.

We have found in our previous work^{10,11} that the steady state of the vortex surface is a promising candidate for such an attractor in phase space. At first sight, it appears that these steady vortex surfaces have some local degrees of freedom, corresponding to the arbitrary shape of the surface, as long as the velocity gap satisfies certain integral equations, following from the minimization of the Hamiltonian.

Initially, we speculated that these surface degrees of freedom were described by some version of a solvable string theory.¹¹ There are two kinds of surface degrees of freedom: the surface shape and the internal metric on this surface, described by the Liouville field.

The shape of the surface was assumed frozen in the turbulent flow in,¹¹ and the remaining internal metric was assumed to be responsible for the multi-fractal scaling laws for the moments of velocity circulation.

The new recent understanding eliminated the shape of the surface as degrees of freedom while placing no restrictions on the internal metric on this surface.^b

Some surfaces are "more equal" than others because they are stable at the microscopic level. These are the CVS surfaces satisfying the stability equations (1).

It is truly remarkable that such a simple equation, involving just three letters, leads to such a multitude of very specific consequences for the turbulent flow. These equations, combined with the usual equations of hydrostatics, allowed us to compute the shape of the surface and its velocity field.

The vorticity is pressed into the surface from both sides by negative normal strain, leading to a narrow Gaussian profile of vorticity in the normal direction. The width of this boundary layer goes to zero as some negative power of Reynolds number in the turbulent limit.

We assume that our flow and the surface are subject to a constant strain, a random traceless matrix created by a multitude of other vortex structures located far away from this one. Such random strain is described by eigenvalues $p + q, p - q, -2p$ adding up to zero. The parameters p, q are distributed by a Gaussian

^bthe Liouville degrees of freedom are still there, but they do not influence the biggest effects we are studying here.

multiplied by a famous Vandermonde determinant, which is $|q||q^2 - 9p^2|$.

The normal strain is uniform all around our vortex surface $S_{nn} = 2p$, so that at $p < 0$ we have one of the stability criteria fulfilled. The tangent strain is degenerate: there is zero strain along the tangent velocity gap.

The energy dissipation occurs at the surface, and we have proven that this surface integral is conserved in the Navier-Stokes dynamics in the turbulent limit.

Let us stop and think about this conservation law. This is *not* an Euler conservation law, violated by viscosity, like the energy conservation. We have found a previously unknown Navier-Stokes conservation law, and it comes about as a result of exact cancellation of the vortex stretching and diffusion terms in the Navier-Stokes equation used for the time derivative of the enstrophy.

The Euler dynamics would lead to an explosion of enstrophy were it not offset by the diffusion in full Navier-Stokes equation. For any other vortex surface but the CVS the diffusion would overcompensate vortex stretching so that the notorious energy dissipation constant \mathcal{E} would slowly drift to zero.

The Kolmogorov theory kept this skeleton in the closet for 80 years. The basic constant of the theory was not constant after all. Better to say, it *was* constant, but nobody knew why.

As we see it now, \mathcal{E} is conserved because of the CVS stability of the vortex surfaces hidden behind the rough picture of the energy flow in Fourier space. The shape of the discontinuity surface cannot be described by a finite (or even convergent) set of Fourier coefficients of the velocity field – it is like describing the smile of Mona Lisa by the spectral analysis of the paints used by Leonardo.

True, the energy flows from large scales and dissipates in small scales in thin boundary layers of the CVS surface, but this spatial picture is very different from the hierarchical cascade of energy "from a big eddy to a smaller one".

On the other hand, the conservation of energy dissipation on the CVS surface makes this parameter an appropriate scaling factor for the K41 theory viewed as dimensional analysis without vindicating the scenario of the energy cascade in physical space.

The K41 energy spectrum undeniably exists at least at medium Reynolds numbers when the vorticity has not yet collapsed into the vortex surface.

Let us come back to our exact solution.

The velocity field and the surface shape were computed exactly in quadrature using the parametric equation in a complex plane ζ . The cross-section is a conformal map $C(\zeta)$ of the unit circle $|\zeta| = 1$ into the physical space, whereas the complex velocity field in the xy plane is given by another conformal map $V(\zeta)$.

The dissipation PDF reduces to integrals involving these algebraic functions. We computed these integrals numerically and plotted the PDF (Fig. 4).

The solution for arbitrary p, q in stable region $-q < p < 0$ describes a hollow vortex tube, much larger than the viscous scale. All vorticity confines to the boundary layer; the width of this layer is going to zero as a positive power of

viscosity in the turbulent limit.

The cross-section of our hollow tube has an oval shape, with seams on four sides (Fig 7,8).

Hollow vortex tubes were observed in the recent DNS,¹² but it is hard to tell until some research would specifically hunt for hollow tubes in turbulent flow simulations.

The flow is forced by a tensor force, with a constant random strain tensor, distributed as a Gaussian random traceless matrix.

The origin of this random force is the accumulation of a large number of $1/R^3$ tails of the Biot-Savart laws for other remote vortex surfaces with random locations and random directions of the net vorticity.

The sign of the flow is fixed by the stability, coming from the microscopic analysis of the Navier-Stokes equation in a boundary layer.

The same requirement follows from the Kelvin-Helmholtz stability of the vortex surface.

This stability condition $S_{nn} < 0$ is the origin of the flow's irreversibility. We choose the parameters so that the energy dissipation (and equal energy pumping) stays finite in the limit of vanishing viscosity.

We considered the dilute gas of these closed vortex surfaces (vortex bubbles), with a large mean distance between bubbles, compared to their size.

In this dilute gas approximation, we derived the Gaussian random strain from an infinite number of remote vortex structures, adding to the Biot-Savart formula for the strain at large distances and averaging to the random constant stress tensor due to the Central Limit theorem.

This calculation leads to a self-consistency relation (65) for the variance of the random strain, which then leads to a new scaling law for the length of the cylindrical surface $L \sim \nu^{-\frac{1}{2}}$ in the turbulent limit.

We computed with high precision all coefficients in these scaling relations for our cylindrical solution (65).

Using exact solution⁵ and the dilute gas approximation, we computed the PDF for the energy dissipation in closed form(39), plotted in log-log scale at 4. This curve is universal in our solution; there are no model approximations nor any dimensionless parameters.

In the same way, one can compute the distribution of the circulation and other observables, such as the Wilson loop $\left\langle \exp \left(i \gamma \oint_C v_\alpha dr_\alpha \right) \right\rangle$.

The reader may wonder what is the relation between these unique CVS surfaces and random surfaces of the string theory, which we recently suggested to apply to the Turbulence problem.¹¹

The answer is that the hardest part of the string theory— random shape of the vortex surface is now gone, but some other parts are still relevant.

As it was advocated in,¹¹ the Gibbs statistics of vortex structures involves soft degrees of freedom on the vortex surface, related to its internal metric. The physical

meaning of this internal metric is the transverse motion of the fluid along the surface, without changing its shape.

Within the vortex sheet dynamics, such motions lead to re-parametrization of the surface. The invariant part of these re-parametrizations is given by the conformal metric, obeying the dynamics of the 2D string theory.^{14,15}

This metric is described by a 2D Liouville field, which may be the source of the multi-fractal scaling laws. The current classical theory of a steady vortex sheet, strained by a random tensor, would not explain these laws.

We have to modify this string approach to the Gibbs statistics of the vortex sheets to accommodate the newly found conservation of the anomalous dissipation on the surface.

This surface dissipation integral can now become the effective Hamiltonian in Gibbs statistics.

Conserved effective Hamiltonian is necessary for the stationary Gibbs distribution, and now we have such an effective Hamiltonian.

The fluctuating shape of the vortex surface is replaced by the CVS shapes, which are rigidly related to the background strain. Still, the Liouville degrees of freedom on this rigid surface may play an important role in the low-temperature statistics.

The conservation of the surface integral (30) holds for *arbitrary* internal metric g_{ab} on this surface. Therefore, this integral is not a number but rather a parametric invariant functional of internal metric, conserved in the Navier-Stokes dynamics.

Another soft degree of freedom is the fluctuation of the discontinuity Γ around the stable background given by CVS.

Such theories were considered before, and they are described as a $c = 1$ string theory in a background target space.^{14,15} In our case, this background space is the CVS surface.

The merging of these two approaches is becoming our next project.

Acknowledgments

I am grateful to Sasha Polyakov, Pavel Wiegmann, and the Max Planck Institute seminar participants for stimulating discussions of this work.

The help from Arthur Migdal with *Mathematica*[®] is also greatly appreciated.

This work is supported by a Simons Foundation award ID 686282 at NYU.

References

1. J. Burgers, A mathematical model illustrating the theory of turbulence, in *Advances in Applied Mechanics*, eds. R. Von Mises and T. Von Kármán (Elsevier, 1948) pp. 171 – 199.
2. A. A. Townsend, *Proc. Roy. Soc. Lond. Ser. A.* **208(1095)**, 534–542 (1951), doi:10.1098/rspa.1951.0179.
3. A. Migdal, *Physics of Fluids* **33**, 035127 (2021), <https://doi.org/10.1063/5.0044724>, doi:10.1063/5.0044724.

4. K. Shariff and G. E. Elsinga, *Physics of Fluids* **33**, 033611 (2021), <https://doi.org/10.1063/5.0045243>, doi:10.1063/5.0045243.
5. A. Migdal, Confined vortex surface and irreversibility. 1. exact solution for the flow (2021), [arXiv:2103.02065](https://arxiv.org/abs/2103.02065) [physics.flu-dyn].
6. A. A. Migdal, Random surfaces and turbulence, in *Proceedings of the International Workshop on Plasma Theory and Nonlinear and Turbulent Processes in Physics, Kiev, April 1987*, ed. V. G. Bar'yakhtar (World Scientific, 1988), p. 460.
7. M. E. Agishtein and A. A. Migdal, *Physica D: Nonlinear Phenomena* **40**, 91 (1989), doi: [https://doi.org/10.1016/0167-2789\(89\)90029-8](https://doi.org/10.1016/0167-2789(89)90029-8).
8. A. Migdal, Exact algebraic cvs <https://www.wolframcloud.com/obj/sasha.migdal/Published/ExactAlgebraicCVS.nb> (May, 2021).
9. A. Migdal, N dimensional tensor algebra and gradients <https://www.wolframcloud.com/obj/sasha.migdal/Published/NDimensionalTensorMath.nb> (Mar, 2021).
10. A. Migdal, *International Journal of Modern Physics A* **35**, 2030018 (November 2020), [arXiv:2007.12468v7](https://arxiv.org/abs/2007.12468v7) [hep-th], doi:10.1142/S0217751X20300185.
11. A. Migdal, *International Journal of Modern Physics A* **36**, 2150062 (2021), <https://doi.org/10.1142/S0217751X21500627>, doi:10.1142/S0217751X21500627.
12. D. Buaria, A. Pumir, E. Bodenschatz and P. K. Yeung, *New Journal of Physics* **21**, 043004 (Apr 2019), doi:10.1088/1367-2630/ab0756.
13. S. Johnson, Cubature (multi-dimensional integration) (Jul 2017).
14. I. Klebanov, String theory in two dimensions (1991), [arXiv:hep-th/9108019v2](https://arxiv.org/abs/hep-th/9108019v2).
15. A. Zamolodchikov and A. Zamolodchikov, *Nuclear Physics B* **477**, 577–605 (Oct 1996), doi:10.1016/0550-3213(96)00351-3.

10. Figures

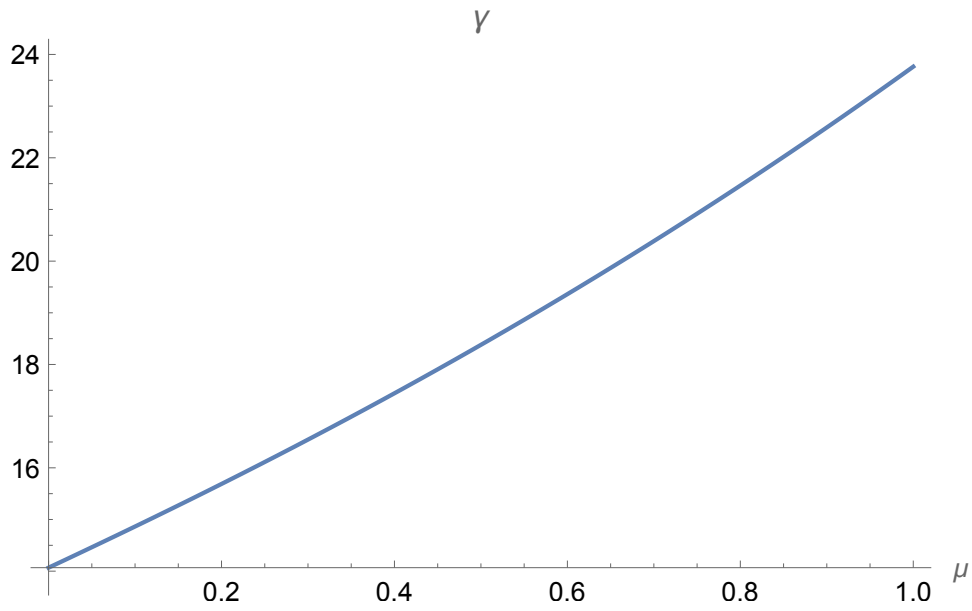


Fig. 1. The circulation γ vs μ .

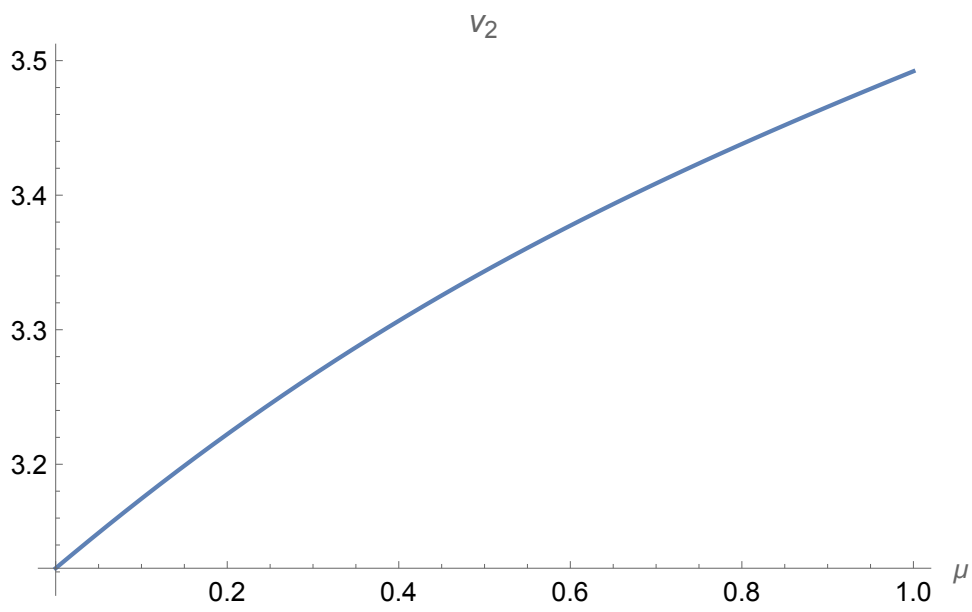


Fig. 2. The parameter v_2 vs μ .

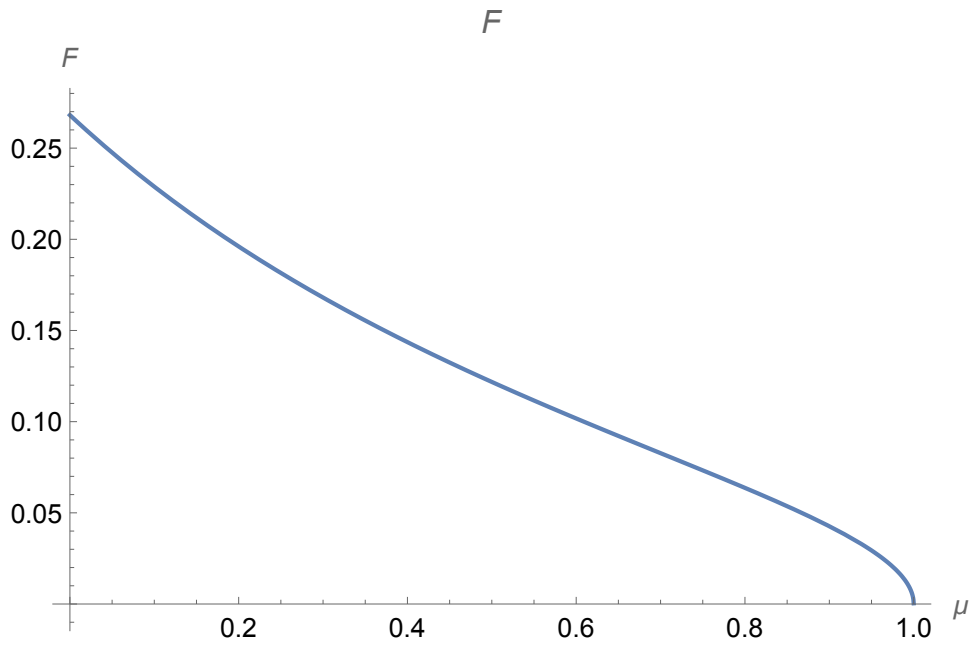


Fig. 3. The universal function $F(\mu)$.

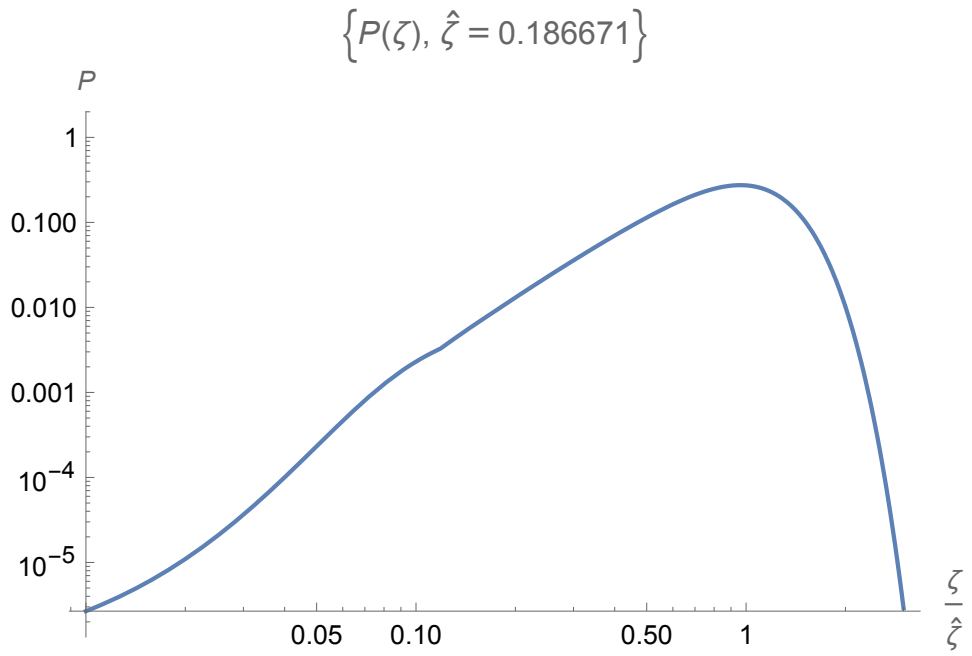


Fig. 4. The energy dissipation PDF in log-log scale

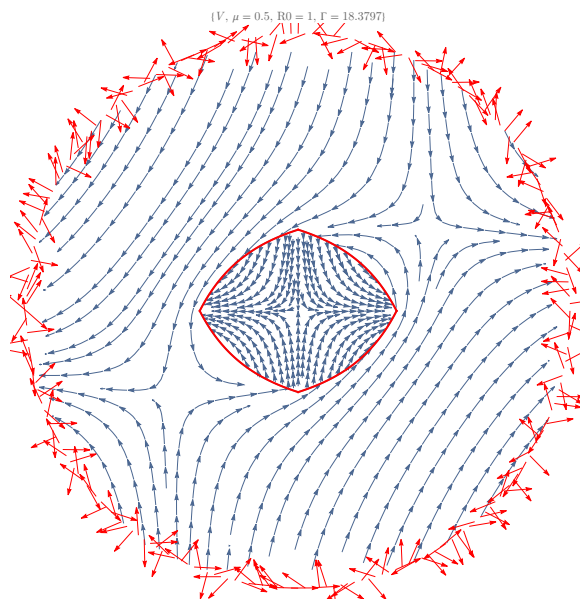


Fig. 5. The flow in the background strain from remote vortex blobs

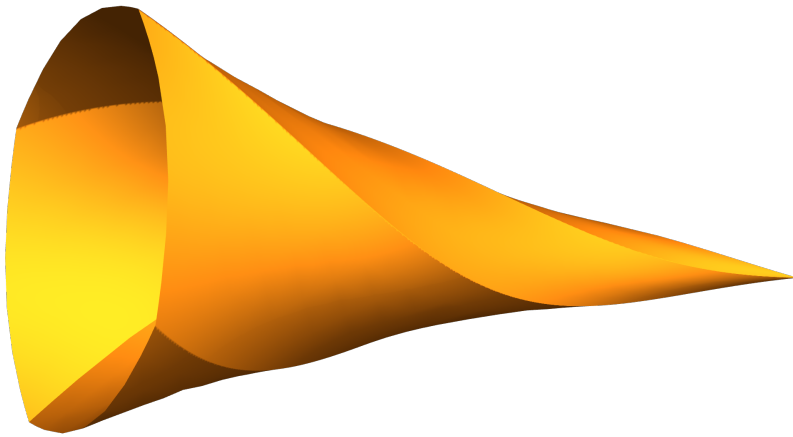


Fig. 6. The vortex surface in slowly varying background strain

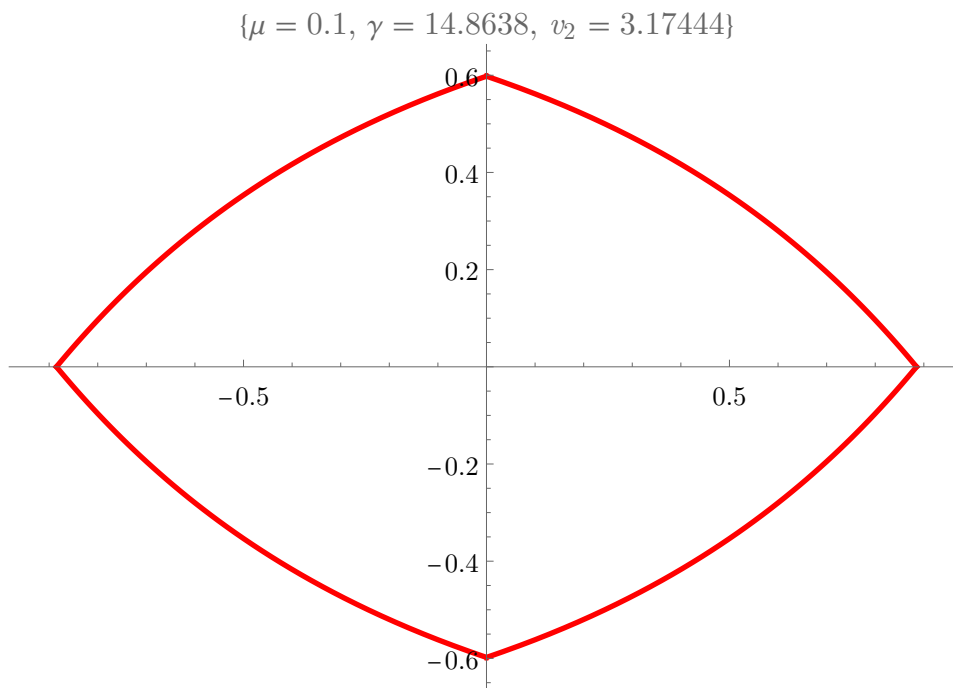


Fig. 7. The vortex surface profile for $\mu = 0.1$

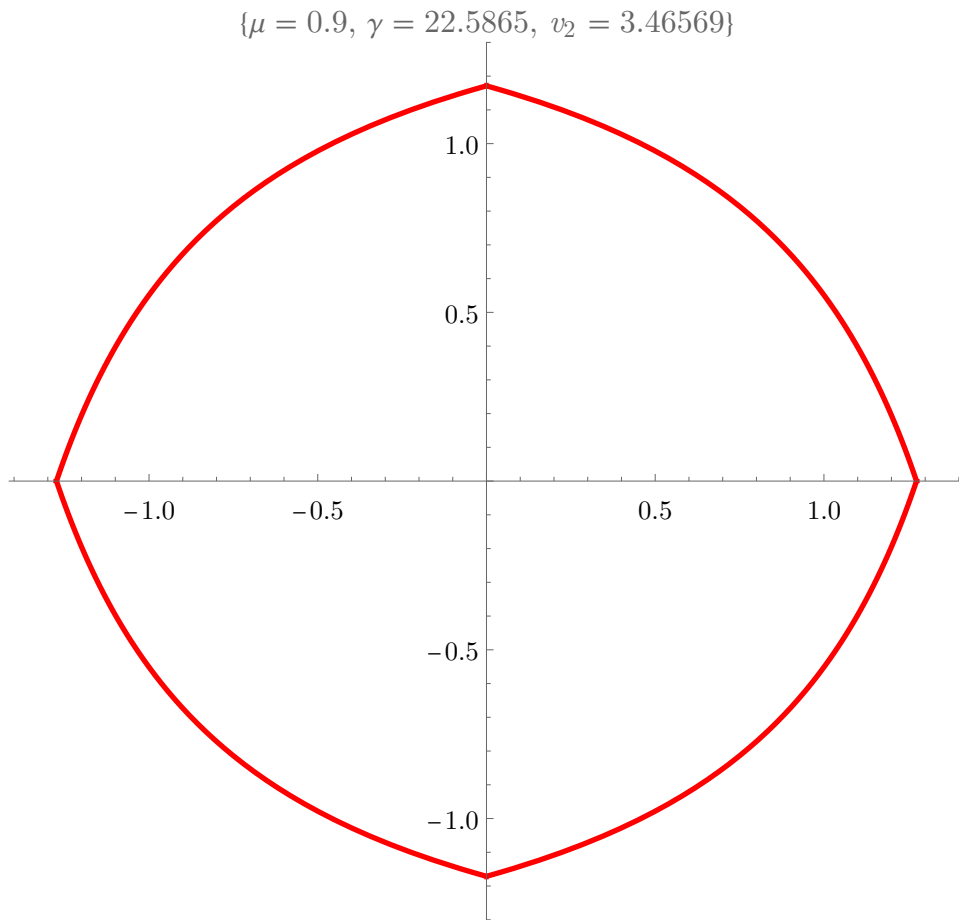


Fig. 8. The vortex surface profile for $\mu = 0.9$